Interaction of Water Spray with Flame

Sourav Sarkar, Joydeep Munshi, Santanu Pramanik, Achintya Mukhopadhyay and Swarnendu Sen

Abstract Increasing concerns about the role of halons on the depletion of ozone in the stratosphere have led to a search for alternate agents for suppression. Water, sprayed in the form of tiny droplets, has emerged as a potential fire suppressant. The present chapter presents a brief review of the recent studies on flame water spray interaction. The effects of water spray on both premixed and non-premixed flames are discussed. The significance of droplet size in flame suppression is explained in details. This understanding will lead to efficient atomizer design for fire suppression systems.

1 Introduction

Fire hazard is one of the major catastrophes that can cause a great damage to property and loss of life. It can occur in all three spaces—above land in a skyscraper, on the ground in the forest; below the ground in mines. Fire protection and safety research

S. Sarkar
Department of Mechanical Engineering, Jadavpur University, Kolkata 700032, India
e-mail: souravsarkar.iitm@gmail.com

J. Munshi
Department of Mechanical Engineering and Mechanics, Lehigh University,
19 Memorial Drive, West Bethlehem, USA
e-mail: jom317@lehigh.edu

S. Pramanik
Mechanical Engineering Department, Indian Institute of Science, Bangalore,
Bengaluru 560012, India
e-mail: santanupramanik07@gmail.com

A. Mukhopadhyay · S. Sen (✉)
Mechanical Engineering Department, Jadavpur University, Kolkata 700032, India
e-mail: sen.swarnendu@gmail.com

A. Mukhopadhyay
e-mail: achintya.mukho@gmail.com

A. K. Runchal et al. (eds.), *Energy for Propulsion*, Green Energy and Technology,
https://doi.org/10.1007/978-981-10-7473-8_7

becomes a major concern due to rapid urban growth in present time. Fire research and development groups have been founded to address industry challenges in multiple areas, including detection and signaling, hazardous materials, electrical safety, fire suppression, storage of commodities, and fire-fighter protective clothing and equipment, among other issues. After Second World War, research in fire safety science increased greatly. However, fire suppression using water spray does not receive much attention due to extensive application of Halon gases. Increasing concerns about the role of halons on depletion of ozone in the stratosphere have led to a search for alternate agents for suppression. A dramatic change happened in the research trend when Halon 1301, Halon 1211 and Halon 2402 were announced illegal in developed countries under the Montreal Protocol (1987).

Waster mist system is widely used as fire extinguishment agent in building and compartment fire. Water sprinkler systems are commonly in engine room, machinery space, electronic equipment rooms and computer rooms. In recent time water mist technology has become one of the major interest of the research community in ships and aircrafts application due to availability, low cost and less storage space. In recent times fire suppression using water spray has been adopted as a technique to mitigate fires related to hydrogen in nuclear power plants. Fine sprays can be used along with the igniters in order to quench the flame when hydrogen concentration is below a threshold limit.

Water spray has emerged as a potential fire suppressant due to its enhanced thermal and physical properties. Water possesses several advantages like non-toxicity and environment friendliness. The physical properties like high specific and latent heats ensure that a small quantity of water can be used for extinguishing the fire. It has high heat capacity and latent heat of vaporization. 418 kJ of heat is required to raise the temperature of 1 L of water from 0° to 100 °C and further 2257 kJ is required to convert it from water to vapor. Water spray helps in suppressing fire in two ways:

1. Water droplets are efficient fire suppressing agent because of its rate of evaporation and high latent heat of evaporation, hence while interacting with the flame, it can absorb heat from the flame reducing the flame temperature. If the flame temperature is below the activation temperature, the flame cannot sustain itself.
2. When droplets vaporize water vapor gets added to the continuous phase displacing oxygen inside the reaction zone of the flame; hence it reduces the local equivalence ratio of the reactant mixture. Eventually, if the equivalence ratio becomes less than the lower flammability limit, flame extinction can occur.

2 Quantitative Characterization of Water Spray

The size of the water droplet is an important parameter that determines the effectiveness of the spray by directly affecting the heat transfer and evaporation. The dynamics of the droplets, that are influenced by the kinetic energy (~d^3) and the aerodynamic drag (~d), are also dependant on the diameter. The size of the droplets vary with the

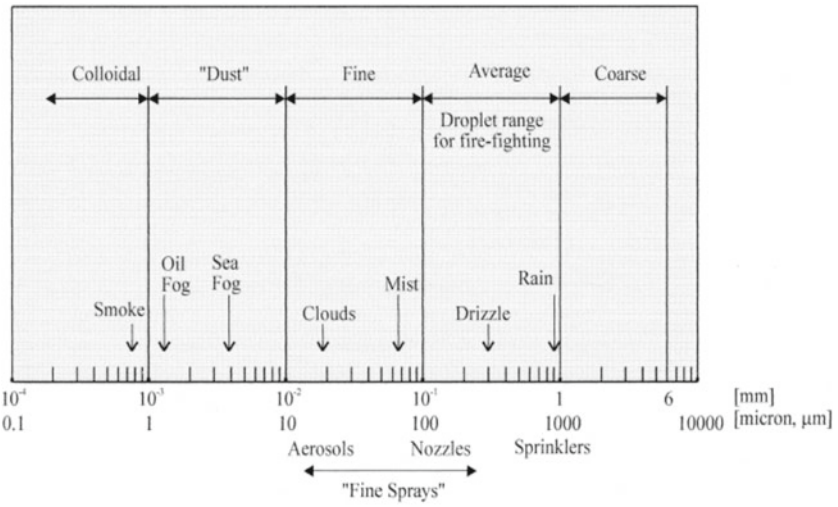

Fig. 1 Classification of droplets based on the diameter. The text below the x-axis shows the range defined as 'fine sprays', together with the approximate locations of 'aerosols', 'nozzles' and 'sprinklers' in the droplet spectrum [1]

mode of generation suited for a particular application and can be divided into several classes as shown in Fig. 1. While distinct boundaries exist for different classes of droplets, the boundary between 'sprays' and 'mists' is somewhat arbitrary. A droplet distribution with a mean diameter of 80–200 μm and a D_{V99} less than or equal to 500 μm has been reported as mist in the literature [1]. The size categories where the 'average' droplet diameter ranges from 100 to 1000 μm is the zone of interest for fire extinction.

Monodisperse droplets are very rare in practical applications as it requires an expensive droplet generator. Hence, practical sprays are mostly polydisperse in nature containing a wide distribution of droplet diameters. Several measures of droplet diameter have been introduced in the literature that represents some physical attribute of the spray as a whole. A standard notation for defining droplet diameters has been suggested by Mugele and Evans [2].

$$D_{mn} = \left(\frac{\sum D^m}{\sum D^n} \right)^{\frac{1}{m-n}}$$

The most commonly used measures of droplet diameters are the mean diameter (D_{10}) and the Sauter mean diameter (D_{32}). For the normal mean diameter, $m = 1$ and $n = 0$; for the Sauter Mean Diameter, $m = 3$ and $n = 2$. Hence, the magnitude of the Sauter Mean Diameter is expected to be higher than the Normal Mean Diameter. The Sauter Mean Diameter (SMD) is the ratio between the sum of the droplet volumes and the sum of the droplet surface areas in a spray. It signifies a particular droplet

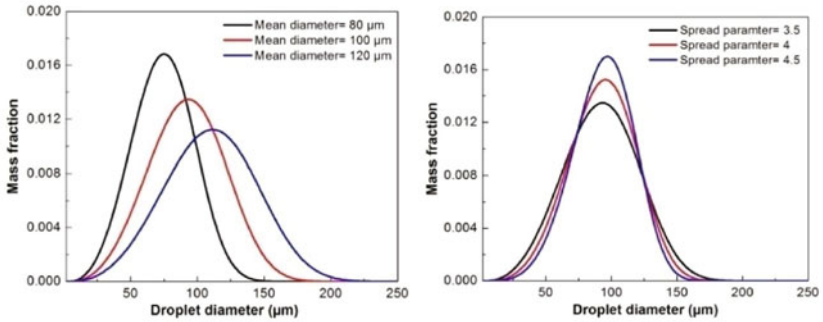

Fig. 2 Droplet distributions different mean diameter and spread parameter for same droplet range

which has the mean volume and surface area for the whole spray. The volume median diameter is another commonly used representative diameter. The number of droplets having diameter lesser than the Volume median diameter is half of the total number of droplets.

Along with the mean diameter, droplet diameter distribution is also an important characteristic of any spray. The empirically obtained diameter distribution in a spray can fit with different mathematical functions. The most popular one is Rosin-Rammler distribution and is given by:

$$Y_d = e^{-(\frac{d}{\bar{d}})^n}$$

Here, Y_d is the mass fraction of droplets of diameter greater than d, $\boldsymbol{d}$ is the mean diameter and n is an exponent known as the spread parameter. Figure 2 illustrates the effect of the mean diameter and the spread parameter on the droplet distribution.

3 Premixed and Non-premixed Flames

Flames can be broadly classified into two types depending on the mixing between the fuel and the oxidizer: premixed flames and non-premixed (or diffusion) flames. Sometimes another type of flame known as partially premixed flame can also be observed which is intermediate to the above two types mentioned. Non-premixed flames occur where fuel and oxidizer enter through different inlets into the combustion chamber and combustion takes place at the stoichiometric mixing plane. Once ignited, a non-premixed flame will situate itself somewhere between the fuel and oxidizer streams in order to satisfy the stoichiometry requirement. Hence, the flame in case of non-premixed combustion is always stoichiometric in nature. This type of flame is also named as diffusion flame as the reaction rate is generally determined by the mixing caused by diffusion [3]. Several examples of diffusion flames can be observed such as the burning of match sticks, candles, lighters, diesel internal

combustion engines etc. Premixed flames, on the other hand, are more like a wave-phenomenon. In this case, the oxidizer and the fuel are homogeneously mixed prior to ignition. Once ignited, the flame starts propagating with a finite speed towards the unburnt reactant mixture. This speed of propagation is known as the flame speed which is a function of the transport properties and the reaction kinetics. In its way of propagation, the flame consumes the unburnt reactant to sustain itself.

3.1 Non-premixed Flame

Several canonical configurations for non-premixed flames exist in the literature that greatly simplifies experimentation and validation of numerical models. One such configuration that has been studied extensively to investigate the physics of flame and water spray interaction is the counterflow diffusion flame. In this configuration a pure diffusion flame is established near the stagnation region of the two opposing jets: the fuel and the oxidizer. The counterflow diffusion flames can be divided into two groups: (1) the counterflow diffusion flame between two opposed gaseous jets of fuel and oxidizer, and (2) the counterflow diffusion flame established in the forward stagnation region of a porous burner [4]. The configurations pertaining to the different counterflow burners are presented in Fig. 3. Counterflow diffusion flames are essentially two-dimensional planar flames that can be reduced to one-dimension by a similarity transform [4]. This greatly reduces the computational costs associated with the validation of complex kinetic mechanisms with the experimental results. As a result, these flames have been studied extensively for understanding the extinction mechanism and complex chemical kinetics and transport processes. An extensive pool of literature consisting of both theoretical and experimental works exists on the structure and extinction of flat laminar counterflow diffusion flames. Smooke and coworkers [5–12] have computationally and experimentally investigated the chemical kinetics and transport processes in counterflow diffusion flames.

Studies on laminar counterflow flames are also used to model complex turbulent diffusion flames. A turbulent diffusion flame can be imagined as an ensemble of several stretched and curved laminar flamelets [13, 14]. The extinction studies on laminar flames are used to generate a flamelet library as a function of the scalar dissipation which is useful for turbulent combustion simulation.

3.2 Premixed Flame

Now if we consider the flame-stationary reference frame for the premixed flame propagation, then upstream mixture approaches the flame with a speed, which is same as the laminar flame speed (S_u) and temperature T_u, whereas the product mixture leaves the surface with a speed U_b and temperature T_b. From continuity equation, we can realize that, as, across the flame, the temperature is going to increase, the

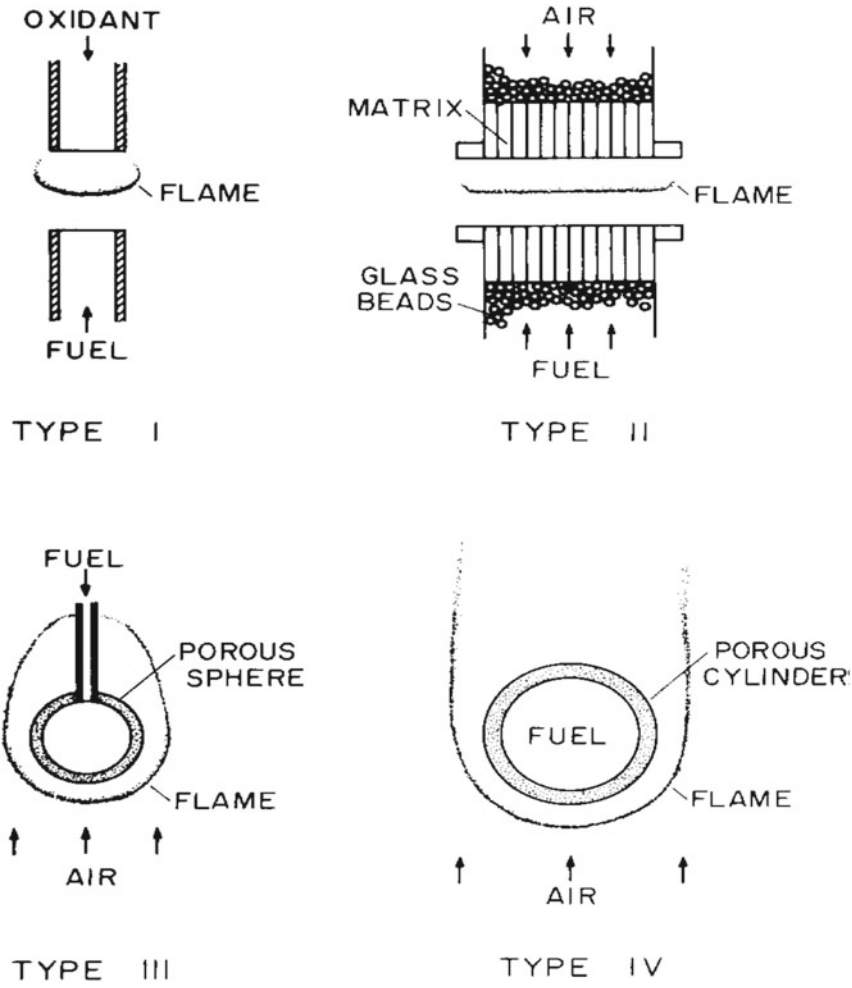

Fig. 3 Different types of counter flow burner [4]

density of the burnt product mixture will be much less than compared to reactant mixture; hence flow acceleration across the flame surface will be observed ($\rho_b \gg \rho_u$; hence $U_u = S_u \ll U_b$). Premixed flame structures can be considered at different levels of analysis. At the hydrodynamic level, premixed flames can be considered as an interface (wave front) across which discontinuities in temperature, species mass fraction, and density can be observed (Fig. 4a). However, these two different fluid dynamic states across the interface are related by the conservation of mass, momentum, species concentration and overall energy. At the flame interface the temperature changes from the reactant temperature (T_u) to adiabatic flame temperature (T_b) and species concentration changes from initial species fraction to zero in the product

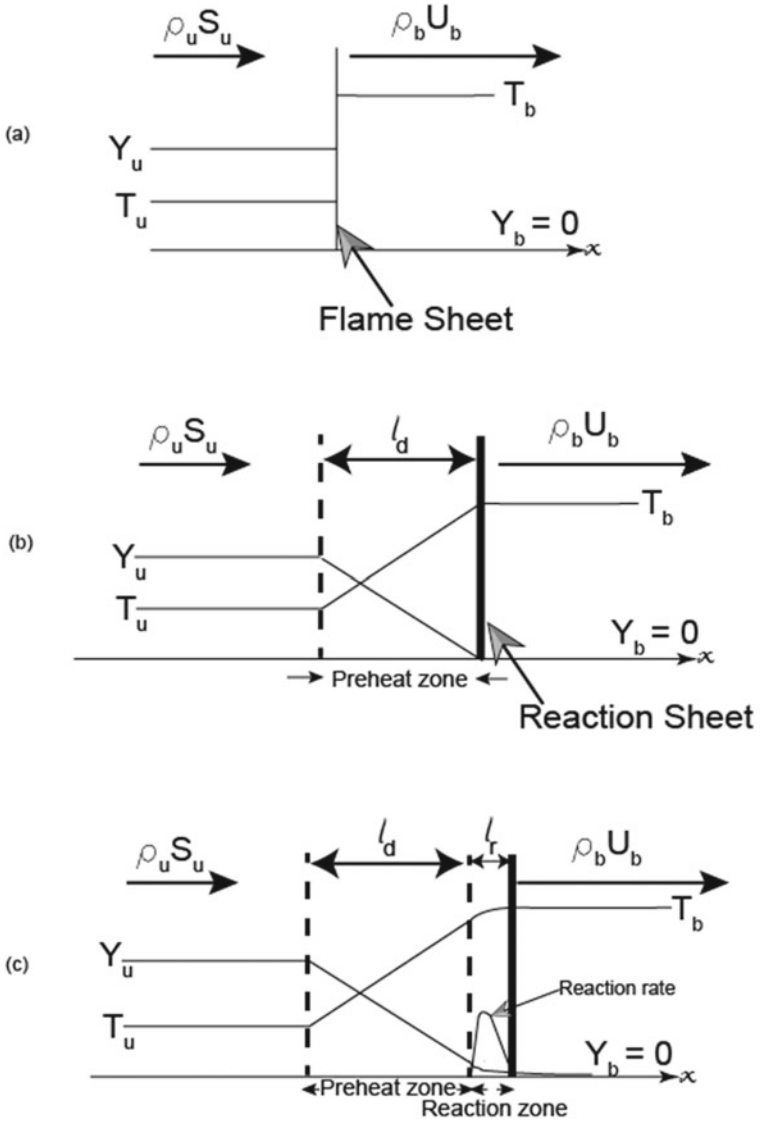

Fig. 4 Premixed flame structure

mixture. In the next level of transport-dominated analysis, the flame interface can be enlarged to get a zone called preheat zone of characteristic thickness l_d (Fig. 4b). The physics here is governed by a balance of heat and mass diffusion. Inside the preheat zone, the temperature gradually increases from reactant temperature T_u to T_b and similarly species concentration decreases from the reactant concentration to zero as shown in Fig. 4b. However, all of the reaction is still taking place in a very thin

sheet like region named as reaction sheet. So, essentially in the preheat zone, we can observe a balance between convective heat and mass transfer and diffusion process. In the third level of analysis, we get a most detailed flame description by enlarging the reaction sheet itself (Fig. 4c). In this region, there is a balance between reaction and diffusion process. So the heat released due to the chemical reaction gets conducted upstream to the preheat zone where reactant heats up and finally reach the ignition point (activation temperature) and chemical reactions take place inside the reaction zone (length scale, $l_r \ll l_d$). It is to be noted that the reaction zone is very small as compared to the preheat zone and even the preheat zone is very small as compared to the whole domain (for example combustion chamber). Usually, preheat zone itself has a few millimeters of length scale. Hence, finally, to conclude, the flame structure can, therefore, be considered to have two distinct zones- preheat and reaction zone. In the preheat zone diffusion process balances with convection of the overall flow field and in the reaction zone diffusion process balances with chemical reaction because of the very high gradient of temperature and species concentration across this region. Overall, across the flame (combining both regions), mass, momentum, species, and energy must be conserved; due to high temperature jump, the density of the mixture reduces and the overall flow field gets accelerated quite a few orders of magnitude (6–7 times for 1800–2100 K if $T_u = 300$ K, less than 1 order of magnitude).

4 Non-premixed Flame and Water Spray Interaction

Flame extinction is considered as one of classical phenomena in combustion studies. Inert gas are often used as diluents for flame suppression. Carbon dioxide and nitrogen are commonly used as inert gas for extinction studies [15, 16]. Lock et al. [17, 18] is studied the effects of CO_2 dilution in fuel and air stream on extinction. Lock et al. [19] investigated the effects of nitrogen dilution and various levels of partial premixing in axisymmetric coflowing jets. Still the use of diluents for fire suppression application are limited to the specific applications due to high storage space and high cost. Water spray is widely applied for fire suppression for its efficient thermal and physical properties. Droplet size of water spray is also important parameter that affects performance of water spray.

4.1 Physical, Thermal, and Chemical Effects of Fine-Water Droplets

Water spray helps in fire suppression through its thermal and chemical effects on the flame. Though the understanding the exact contribution of different effects is not straight forward in large scale fire experiments and modelling. Often laboratory scale flames with a simple configuration such as the counter flow diffusion flame are chosen

for theoretical and experimental study. In those cases, the conventional counterflow flame is modified by the provision for introducing gaseous or condensed-phase agents with the oxidizer stream (Fig. 5). Theoretical or numerical studies often preferred over experimental studies because it allows us to decouple different effects and to perform parametric studies. Lentati and Chelliah [20] numerically have investigated the effects of water spray on methane-air counterflow non-premixed flame based on a hybrid Eulerian–Lagrangian formulation for gas and droplet phase. They have considered mono disperse water droplet of 5–50 μm diameter which is introduced into the air stream of a steady laminar counterflow flame. To observe the physical effect of water vapor air stream with saturated vapor (3.51% by moles or 2.24% by mass) is supplied. 25% of reduction in extinction strain rate is observed due to dilution or displacement of oxygen from air stream due to water vapor addition. Further, same proportion of nitrogen is added instead of water vapor. The effect of this dilution on maximum flame temperature is presented in Fig. 6.

The difference in maximum flame temperature between water vapor and nitrogen dilution is due to different specific heat effects. Addition of water vapor can affect the flame temperature by oxygen displacement and take part in the chemical reactions. It is expected that water vapor can participate in chemical reaction as it has a high three-body collisional efficiency. At sufficient water vapor concentration also it can affect the water gas shift reaction. To isolate the chemical effect water vapor, H_2O is identified as a different compound which did not take part chemical reaction and simulation is performed. It is found from Fig. 6 that the chemical effect of water vapor is negligible.

The contribution of chemical effect is studied for evaporating droplets. It is found from Fig. 7 that the third body recombination effects have a minor contribution in flame suppression. In numerical model, discrete droplet phase interacts with continuous gas phase through source term of mass, momentum, and energy conservation equation. Source term energy conservation equation represents the latent heat of vaporization and increase in the sensible enthalpy of water droplets. To isolate the thermal and chemical effects, four different cases are simulated. In the Fig. 8 symbol (□) denotes when thermal and chemical effects are included. Symbol (Δ) is used to indicate dilution effect when both thermal (inclusion of energy source term) and chemical effects are excluded. In the same figure, symbol (+) and symbol (*) denotes the chemical effects (including dilution and excluding thermal effect) and thermal effects (including dilution and excluding chemical effect) respectively. It was found that extinction strain rate reduces 255–176 s^{-1} due to combined thermal, dilution and chemical effect. If the chemical effect is excluded it drops down to 190 s^{-1}. It is clearly seen that chemical effect has a very small contribution. A reduction of thermal effects is observed for higher droplet size because of incomplete evaporation of larger droplets due to higher evaporation time scale.

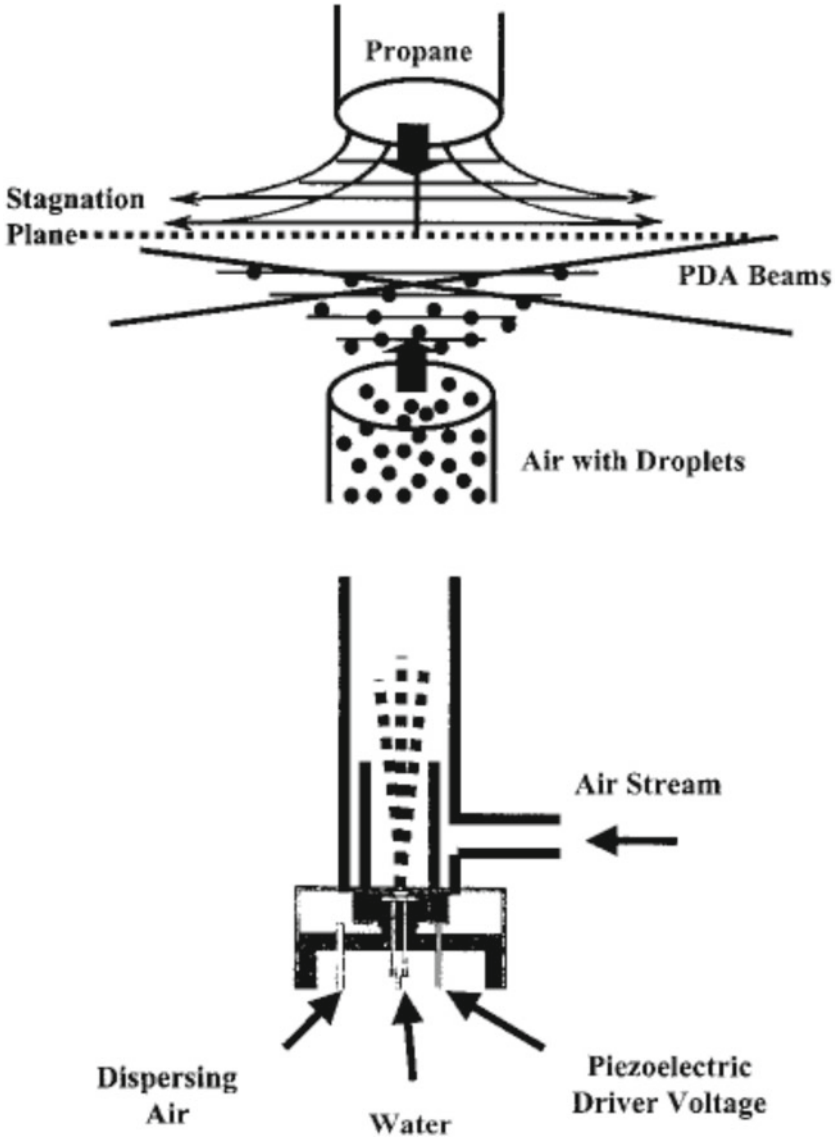

Fig. 5 Experimental setup [21]

4.2 Dynamics of Water Droplets in a Counterflow Field

Droplet size plays a crucial role in flame extinction. Fine water spray is preferred over larger droplets as it can suspend longer period in air than larger droplets. The smaller droplets also have higher surface area to volume ratio than larger droplets

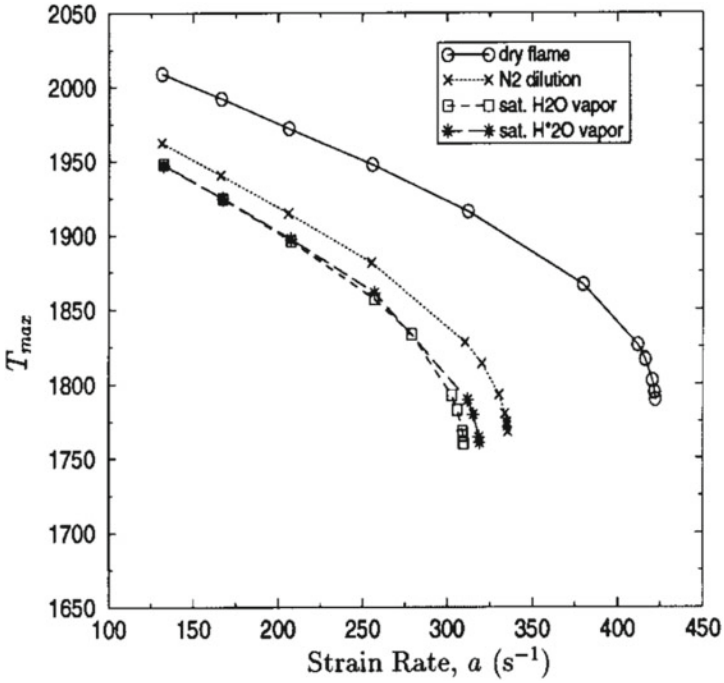

Fig. 6 Comparison of T_{max} versus a, for dry cases (o), diluted cases with saturated water vapor (□), water vapor excluded from chemistry (*), and nitrogen (×) [20]

which enhances the evaporation process. However, it is found that effectiveness of water spray is not solely governed by the surface area. Droplet dynamics near flame region also plays an important role during fire suppression. Larger droplets may not completely evaporate beyond the flame zone reducing the effectiveness of fire suppression. On the other hand, low droplet/gas velocities and/or very small sized droplets may lead to evaporation far ahead of the flame. In such cases, the full quenching potential of the spray is not utilized. Depending on the competition between the residence and evaporation times of the droplets, various flame regimes like oscillatory flames may arise.

Lentati and Chelliah [22] numerically studied the dynamics of water droplets in a counterflow field and their effect on flame extinction. They used a hybrid Eulerian Lagrangian formulation to model gas and droplet phase. Several monodisperse sizes of water droplets ranging 5–50 μm is chosen for simulation. The strain rate is kept 130 s^{-1} in the simulation. Velocity at different axial location presented in the following Fig. 9. It is observed 5 mm droplet completely follow the gas phase velocity due to low inertia where as large droplets significantly deviate from the gas phase velocity. It is also observed that 5 μm droplets completely evaporate before reaching the flame front whereas 50 μm penetrate inside the flame and enter in the fuel side then further reverse its direction. A non-dimensional number referred as Stokes number

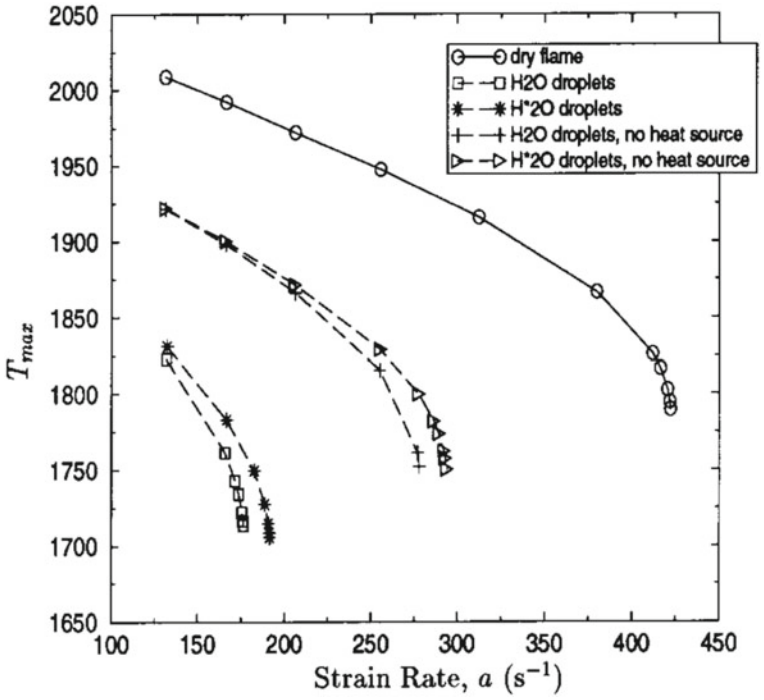

Fig. 7 Comparison of $T_{\max}$ versus a, for dry cases (o) and 2% by mass of 20-μm water droplets, with chemical effects modified (*, Δ) and thermal effects modified (+, Δ) [2]

in the literature is often used to characterize the droplet motion is spatiotemporally varying gas flow field. Stokes number is defined as the ratio of characteristic droplet response time to the characteristic flow time. It is expressed as,

$$St = \frac{\rho_o D_0^2 a}{18\mu_g}$$

where is the ρ_0 droplet density and μ_g is the gas dynamic viscosity. Droplet inertia can be a measure of characteristic droplet response time. Higher the inertia lesser it will deviate from initial trajectory; hence higher will be the droplet response time. Characteristics droplet response time increases with the increase of droplet diameter. So for a constant strain rate, Stokes number increases with the increase of droplet diameter. When Stokes number approaches the value 0.1 the deviation of the droplets are almost negligible. Figure 10 shows the droplet temperature, T_d, of different droplet sizes. It is observed that 5 μm droplet is almost in thermal equilibrium with the gas phase. A small thermal lag is observed for larger droplets. The source term in the gas phase continuous phase continuity equation due evaporation of different

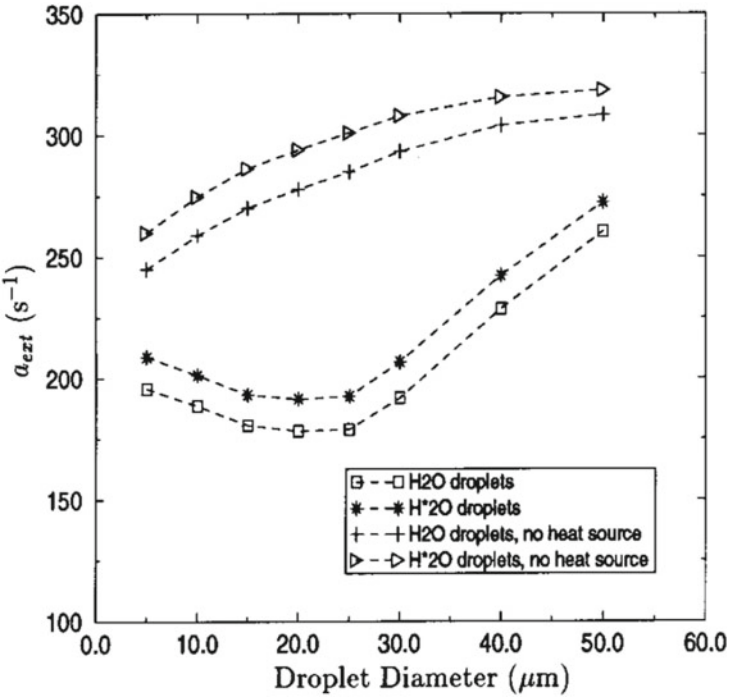

Fig. 8 Variation of extinction strain rate as a function of droplet size, with chemical and thermal effects modified [21]

droplet size is presented in Fig. 11. It is clearly observed that 5 μm droplet completely evaporated before reaching stagnation plane (Figs. 12 and 13).

Zegers et al. [21] have experimentally studied droplet velocity and evolution of droplet number density in the vicinity of the flame zone of a non-premixed counter-flow propane/air flames. Piezoelectrically generated a monodispersed water mists of initial droplet size ranging from 14 and 42 μm is seeded into the air stream to investigate the flame suppression effectiveness. The number density and average velocity of droplet size 30 and 18 μm are plotted versus axial position. It is observed that number density increases initially then starts to drop in front of the flame both 30 and 18 μm droplets. The variation of number density is explained using drag force and evaporation. Gas velocity starts to drop in the axial direction as it approaches the stagnation plane. In this region, droplets start to decelerate which causes a spatial accumulation of droplets and number density increases. The droplets start to move in the radial direction due to diverging flow field at the exit of the lower air duct. Evaporation process also starts to dominate as it approaches flame front. These two reasons cause a rapid drop in number density. It is found that 18 μm droplets completely evaporated after reaching the flame front. Whereas 30 μm droplets have penetrated the flame front and traveled in the radial direction.

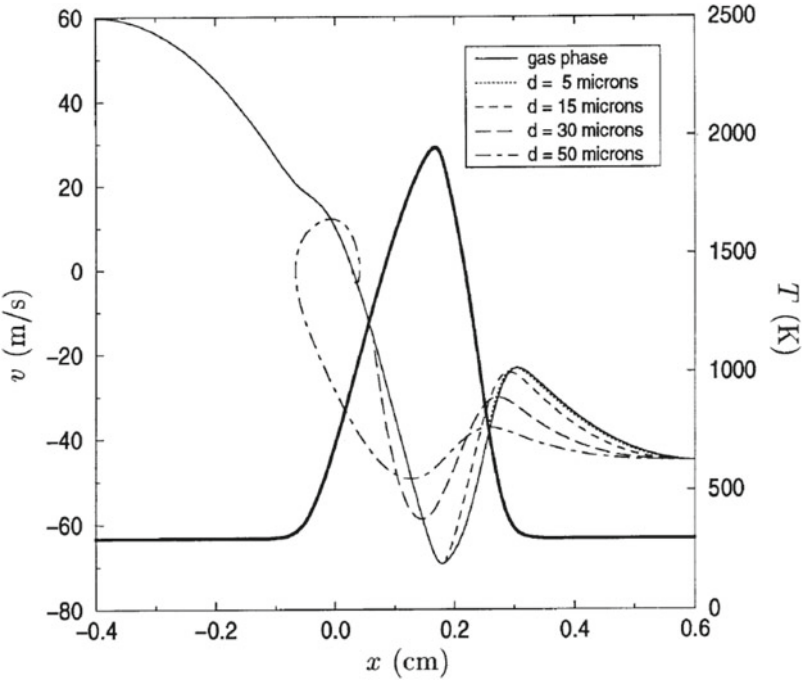

Fig. 9 Comparison of the gas velocity and droplet velocity of different sizes, with droplet source terms turned "off" in gas-phase calculations. Also shown is the gas temperature (thick line) [22]

4.3 Optimum Droplet Diameter

It is clearly understood that droplet size plays an important role in flame suppression. It is observed from the studies that there exists an optimum diameter for a monodisperse spray for which the effectiveness of spray is maximum. In observation can be explained on the basis of comparative effects between vaporization Damköhler number and Stokes number. Vaporization Damköhler number is defined as the ratio of characteristic flow time to vaporization time. It is expressed as

$$Da = K/D_0^2 a$$

where K is the vaporization rate, D_0 is the droplet diameter and a is the strain rate Characteristic flow time can be estimated by the inverse of strain rate. For a constant evaporation rate, vaporization time increases with the increase of droplet diameter. So for a constant strain rate, Damköhler number decreases with the increase of droplet diameter. Stokes number is defined as the ratio of characteristic droplet response time to the characteristic flow time. It is expressed as

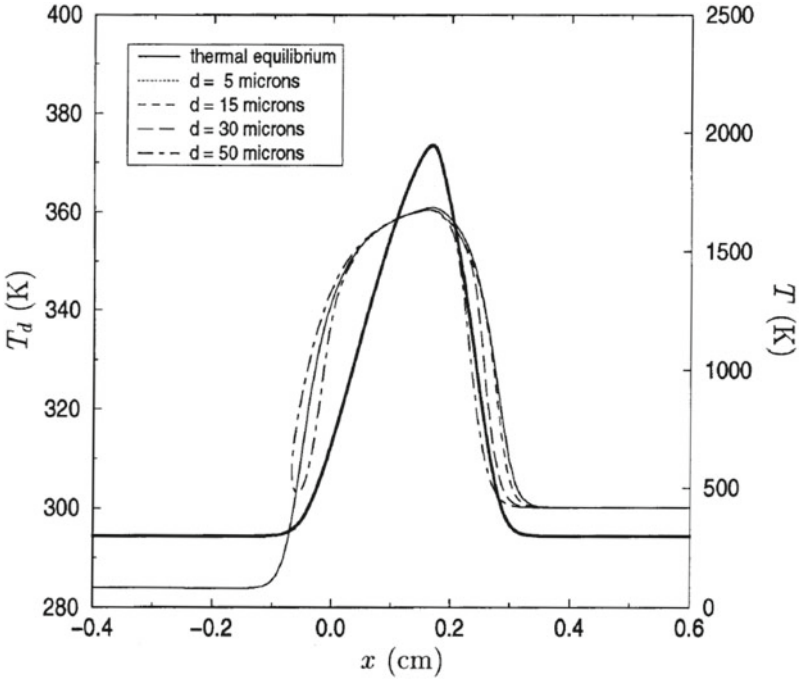

Fig. 10 Comparison of droplet temperature, *Td*, of different droplet sizes, with droplet source terms turned "off" in gas-phase calculations. Also shown is the gas temperature (thick line) [22]

$$St = \frac{\rho_0 D_0^2 a}{\mu_g}$$

where is the ρ_0 droplet density and μ_g is the gas dynamic viscosity. Droplet inertia can be a measure of characteristic droplet response time. Higher the inertia lesser it will deviate from initial trajectory; hence higher will be the droplet response time. Characteristics droplet response time increases with the increase of droplet diameter. So for a constant strain rate, Stokes number increases with the increase of droplet diameter. So higher stokes number will be more preferred due to penetration into the flame and higher Damköhler number will be preferred due to better evaporation. The simultaneous requirement of these to lead to an existence of an optimum droplet diameter. Chelliah [23] investigated the variation of optimal droplet diameter for different water mass loading for counter flow methane air non-premixed flame. 15–20-mm droplets are found to be the most effective. Zegers et al. [21] investigated the effect of 3 different size droplets on a propane air non-premixed flame. They also found an optimum droplet size for more effective flame suppression.

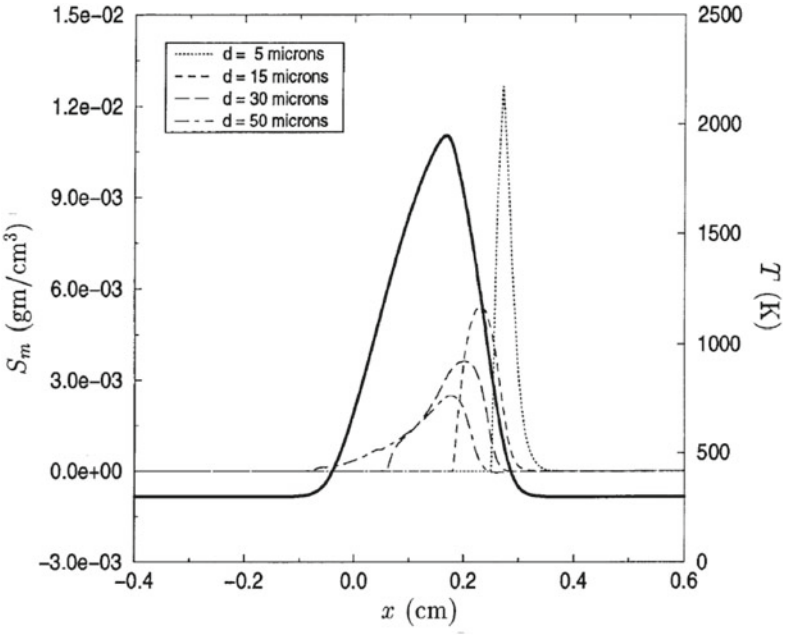

Fig. 11 Typical S_m profiles of different droplet sizes, with $Y_0 = 0.02$ and droplet source terms turned "off" in gas-phase calculations. Also shown is the gas temperature (thick line) [22]

4.4 Effect of Size Distribution of Polydisperse Water Spray

Practical atomizers produce a large spectrum of droplets. The common practice of representing the polydisperse spray by some suitable mean diameter (e.g., Sauter mean diameter) may not be effective in the present situation where the dynamics of the individual droplets are determined by their respective sizes. Dvorjetski and Greenberg [24] investigated the effect droplet size distribution on a counterflow diffusion flame. They considered six initial droplet size distributions for analysis. Three of them have the same Sauter mean diameter and rest of three have the same D_{20}. Three different distributions: (1) a quasi-monodisperse spray, (2) a bimodal spray and (3) a "normal"-spray are considered for both cases. In addition to these, 2 mono-sectional descriptions of the spray are considered for mathematical reference. The first mono-sectional spray has droplet size ranging from 20 to 84.7 and SMD 44.8 μm. The second mono-sectional has a droplet size of 20–80.1 mm and D_{20}= 34.4 μm. The effect size distribution with same SMD on flame temperature is presented in Fig. 14. The maximum flame temperature obtained without water spray is 1570 K. Maximum flame temperature obtained with bimodal water spray and full polydisperse water spray are 1480 K and 1470 K respectively. The quasi-monodisperse spray reduces the flame temperature a few more degree further than full polydisperse water spray. Mono-sectional model of the spray gives the lowest flame temperature.

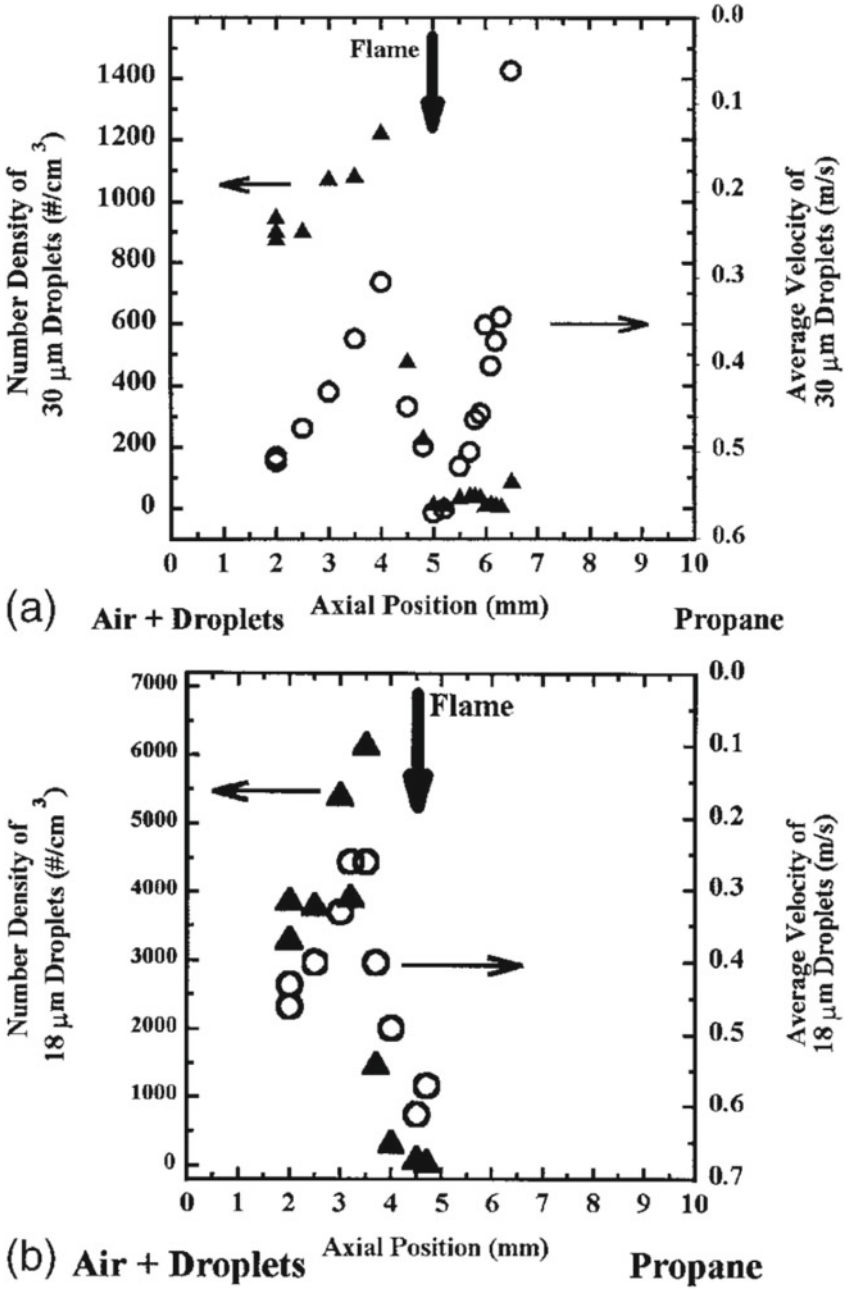

Fig. 12 **a** Profiles of number density (triangles) and velocity (circles) for 30 μm droplets versus location in a 170 s^{-1} strain rate propane/air 30 μm mist counterflow flame. **b** Profiles of number density (triangles) and velocity (circles) of 18 μm droplets versus location in a propane/ air 18 μm mist counterflow flame [21]

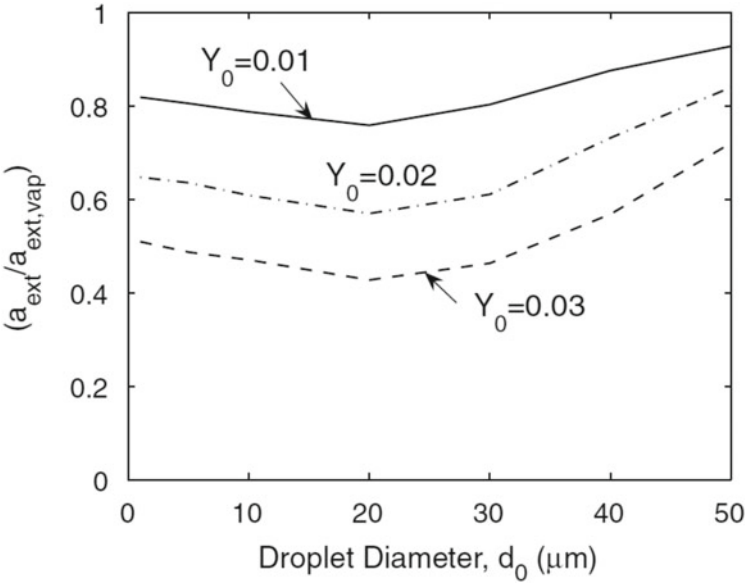

Fig. 13 Variation of the flame strength of a nonpremixed flame versus droplet diameter, for selected water mass fractions Y_0 [23]

Figures 15 and 16 represent the variation of the water mass fraction versus critical strain rate curves for the distributions with same SMD and same D_{20} respectively. It is clear that quasi mono-disperse spray is the most effective among three realistic distribution with same SMD. However full polydisperse water spray is found most effective among three realistic distribution with the same $D_{20.}$ So it can be concluded that representing a polydisperse by a single representative diameter (number mean, Sauter mean, D_{20}) is inaccurate (Figs. 17 and 18).

Pramanik and Mukhopadhyay [25] numerically investigated the effects of polydisperse and monodisperse spray on counterflow diffusion flame. They found that polydisperse spray is more effective than monodisperse spray after a certain droplet diameter. Sasongko et al. [26] experimentally investigated the extinction condition of a counterflow diffusion flame in presence of polydisperse water spray. Extinction condition is obtained by slowly reducing the oxygen concentration in the oxidizer stream. The effect of mean diameter of the polydisperse spray on the oxygen concentration at the extinction is studied experimentally. In the experiment a double cylinder concentric counterflow burner was used. The inner diameter of the burner was 23 mm which was surrounded by a 40 mm diameter outer cylinder. Methane and oxygen diluted by N_2 were supplied from top and bottom inner cylinder respectively. N_2 was supplied from the outer cylinder to prevent the interaction of atmospheric air with the flame. Strain rate was varied by changing the separation distance between the burners. In the present case strain rate of 160 s^{-1} was chosen for study. Water spray

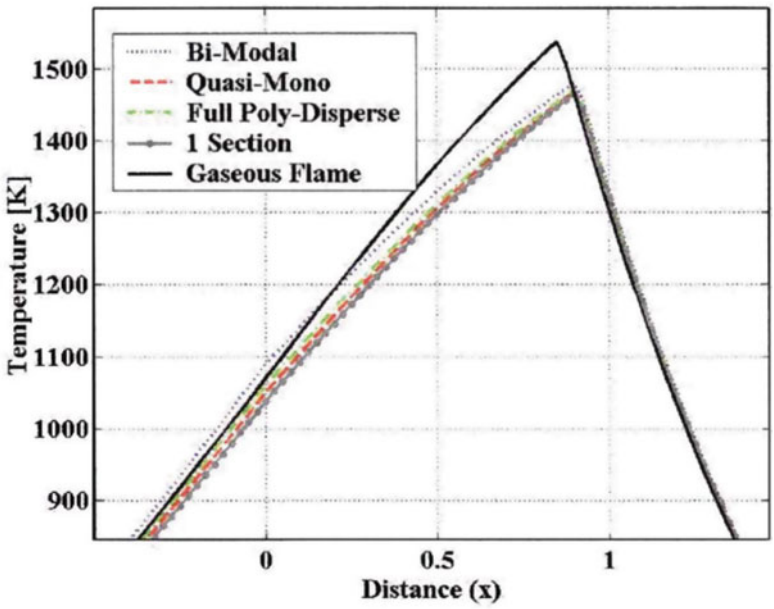

Fig. 14 Comparison of temperature profiles in opposed flow diffusion flames with and without various water sprays present: all sprays have same SMD [24]

produced by a twin fluid atomizer was introduced from the bottom. The atomizing gas flow rate was varied to obtain different droplet size distributions.

The burning behavior of counterflow diffusion flame with water spray for strain rate a = 160 s^{-1} is captured and presented in the figure. Oxygen concentration is varied from 0 and 0.30 to before extinction. Initially, the flame consists of two regions, a yellow luminous region on the fuel side and a blue region on the oxidizer side. The yellow luminous region starts to decrease with the decrement of oxygen concentration as flame temperature reduces. Flame completely turns into blue before extinction. Figure 19 presents the comparison of oxygen concentration at extinction for two different strain rate a = 160 s^{-1} and a = 320 s^{-1}. It is observed that optimum droplet diameter shift in the smaller droplet size with the increase of strain rate. The optimum droplet diameter exists around SMD 65–75 μm at 160 s^{-1} strain rate. For 320 s^{-1} strain rate, optimum droplet SMD lies between 40 and 50 μm (Fig. 20).

Sarkar et al. [27] numerically investigated extinction condition of flat and curved counterflow laminar diffusion flame with polydisperse water sprays. Two dimensional Navier-Stokes equation and energy equations were solved for the gas phase. A reduced reaction mechanism with 16 species and 46 reactions was used to model chemistry of the combustion phenomena. Rosin Rammler distribution was fitted with the experimentally obtained droplet distribution and 1.86 was found as the spread parameter. Discrete phase model with the obtained Rosin Rammler distribution parameters was used for present simulation. The O_2 mass fraction of the

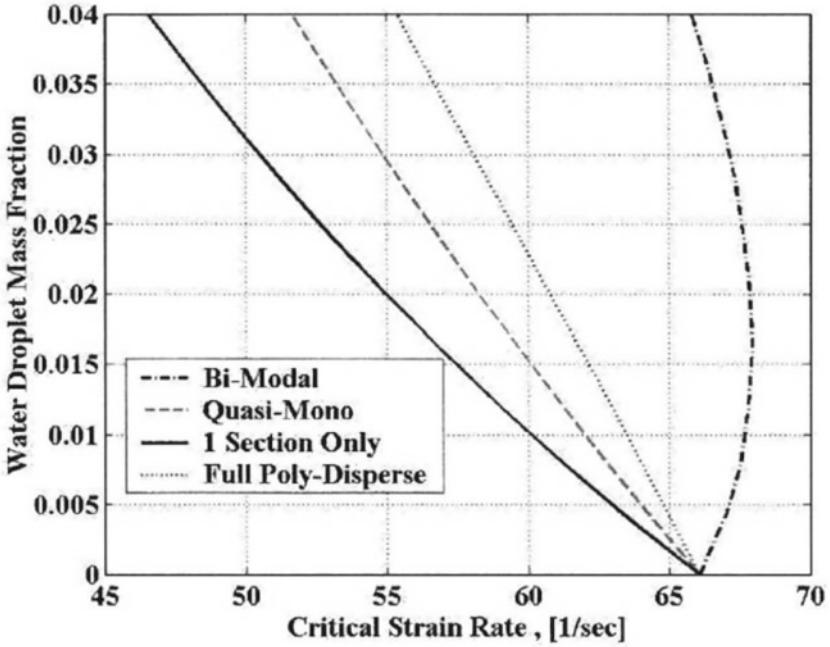

Fig. 15 Comparison of temperature profiles in opposed flow diffusion flames with and without various water sprays present: all sprays have same SMD [24]

oxidizer stream was gradually reduced to obtain the extinction condition. Numerical simulation results were in good agreement with the experimental result reported in Sasongko et al. [26] Approximately 3% deviation was observed from the experimental results of Sasongko et al. [26] in the extinction concentration. The maximum flame temperature and temperature contour of the flame with and without spray at different O_2 concentration are presented in Figs. 21 and 22 respectively.

Yoshida et al. [28] experimentally studied extinction of a counterflow methane/air diffusion flame using polydisperse fine water droplets. A piezoelectric atomizer is used to generate fine water spray. Droplet size distribution and velocities are obtained using Phase Doppler particle analyzer (PDPA). Figure 23 presents the variation of flame thickness with strain rate for different water spray mass loading. In Fig. 23 filled symbol indicate yellow luminous flame and hollow symbol indicate blue color flame. It is observed that flame thickness and flame color significantly change with the application of water spray. Figure 24 presents the velocity of the droplets at different locations for strain rate 80 s^{-1}. It is seen that smaller droplets start to decelerate according to the gas flow at far upstream of the flame front at $y = 14.4$ mm. Closer to the flame front at $y = 8.5$ mm, all the droplets almost move with the same velocity of the gas phase. However, at higher strain rate (230 s^{-1}), droplets velocities

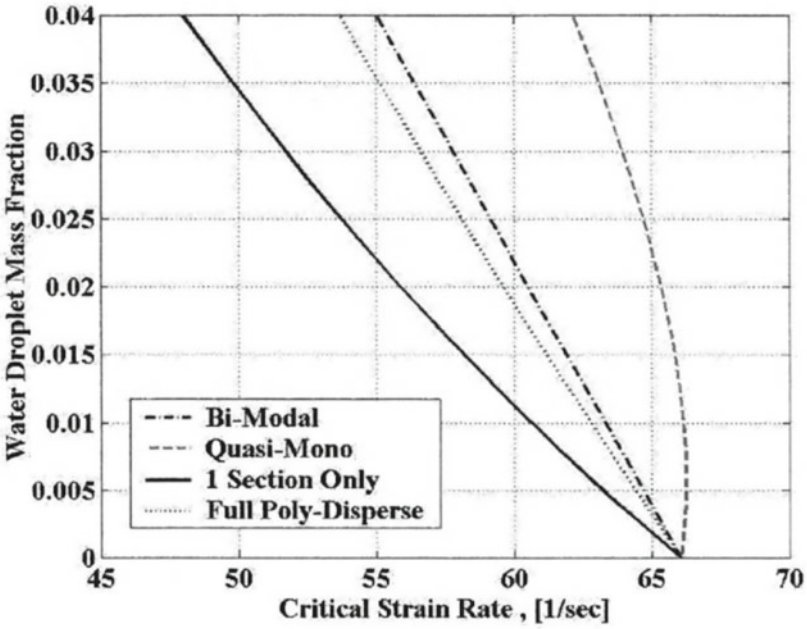

Fig. 16 Comparison of temperature profiles in opposed flow diffusion flames with and without various water sprays present: all sprays have same SMD [24]

are significantly different from gas velocity as high inertia force does not allow to establish equilibrium with the gas phase velocity (Fig. 25).

Lazzarini et al. [29] investigated the role of adding hydroxides of alkali metals to water to enhance the extinction rate. An upper limit of the concentration of alkali metal hydroxide allows one to combine the thermal fire suppression ability of water droplets with chemical suppression ability of alkali metals. Arias et al. [30] numerically investigated the extinction of counterflow non-premixed laminar and turbulent flames with water droplets. Through the analysis of turbulent flames, they demonstrated the role of parameters like flame curvature and local extinction.

Most of the studies referred above are performed with the opposing-jet burners. However there exist few more simple configurations other than counterflow burner for flame water spray interaction study like coflow burner, cup burner etc. Takahashi et al. [31] studied extinguishment of methane and polymethylmethacrylate (PMMA) flame using water spray in cylindrical burner configuration where cylindrical burner is inserted vertically downward into an upward coaxial air stream. The effect of gaseous agents (N_2 and CO_2) and water mist on flame structure and extinction is reported. Ndubizu et al. [32] studied water mist fire suppression mechanisms of a methane air diffusion flame using a modified Wolfhard-Parker burner setup. Liao et al. [33] studied interaction of fine water spray with liquid pool fires.

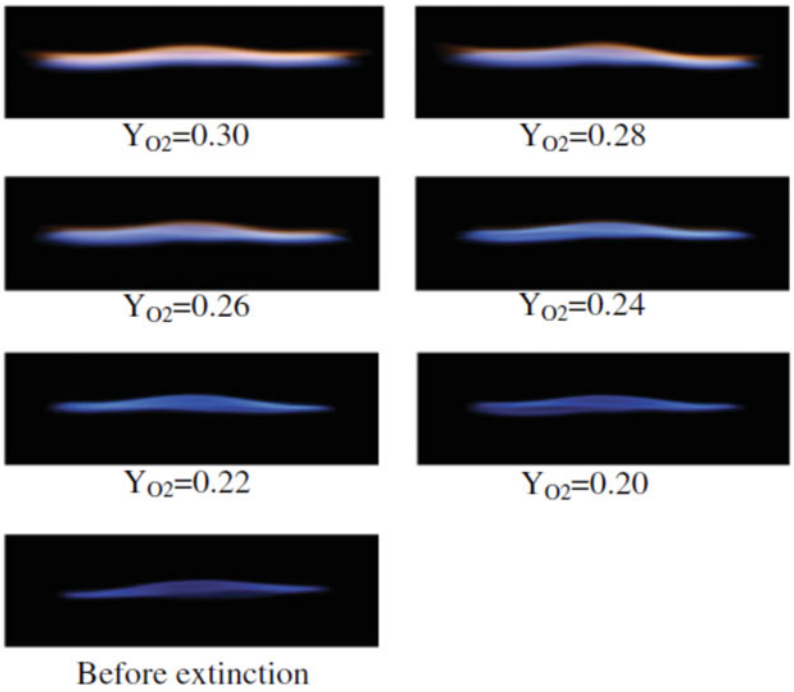

Fig. 17 Photographs of counterflow diffusion flame with water spray for different oxygen concentrations of the oxidizer Y_{O2} (SMD = 97.6 lm, Y_w = 0:022; a = 160 s^{-1}). [26]

5 Premixed Flame and Water Spray Interaction

5.1 Dynamics of Droplets

Chelliah [23] numerically investigated the effects of droplet size on flame inhibition for laminar methane-air premixed flames. Monodispersed droplet size of 10, 20 and 30 μm are chosen for numerical study. Figure 26 shows the variation of normalized droplet diameter for those initial droplet sizes in the flow field. It is observed that smallest droplets completely evaporate in the preheat zone of the flame. Whereas 30 μm droplets completely penetrate inside the flame and continue to evaporate in the post flame region. Gas velocity rapidly increases in front the flame due to thermal expansion. Droplets also start to accelerate due to drag. The response of droplets is presented in Fig. 26. A velocity lag is observed for larger droplets due to higher inertia. The thermal response is presented in Fig. 28. The difference between the droplet and gas phase temperature is minimum for 10 μm droplets. Mass source term due to evaporation for different droplet size is presented in Fig. 29. It is observed that 10 μm droplets completely in preheat zone and flame front. Whereas 30 μm droplets majorly evaporated in the post flame region (Figs. 27 and 30).

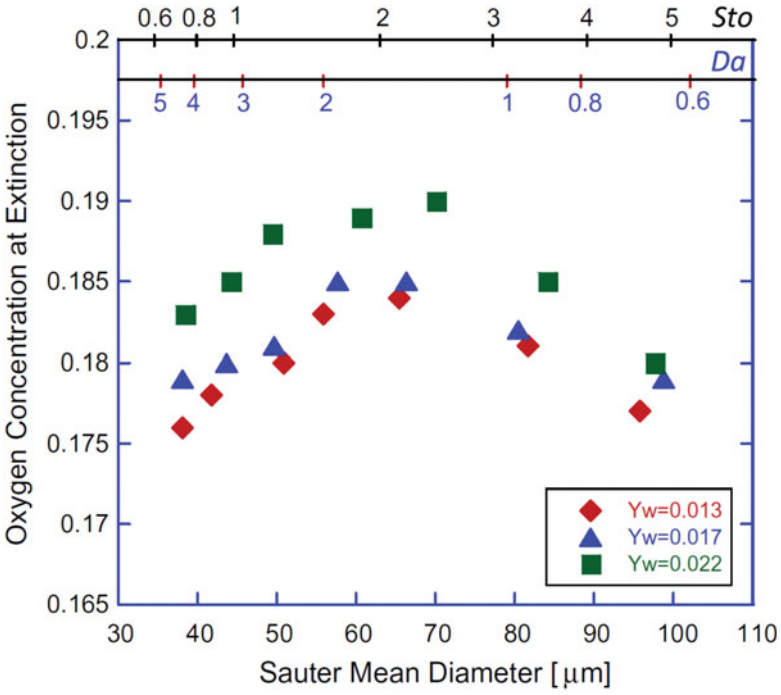

Fig. 18 Dependence of oxygen concentration at extinction on the Sauter mean droplet diameter for different water droplet mass fraction Y_w ($a = 160\ s^{-1}$) [26]

5.2 *Effect on Flame Speed*

Significant flame speed drop was observed due to with the application of water spray. Flame speed decreases with spray mass loading. The maximum decrement of flame speed was obtained for 10 μm droplets. Numerical results also very good agreement with the experimental results.

Yoshida et al. [34] have experimentally investigated the suppressing effect of fine water droplets in propane/air premixed flames in stagnation flow field. They have also found the dependence of laminar flame speed on the stretch rate which is in good agreement with the previously reported data. Laminar flame speed was observed to increase with increasing stretch in absence of any water droplets similar to the study of Law et al. [35] On the other hand laminar flame speed started reducing with increasing stretch rate in presence of fine water spray due to change in the mixture Lewis number and Markstein length (Fig. 31). However, it was not in agreement with the numerical study conducted by Yoshida et al. [34].

It was concluded that flame speed reduction due to mist accumulation at the stagnation plate is larger than the flame speed increment due to the flame stretch, hence providing a net decrease in the flame speed due to water mist addition. It was

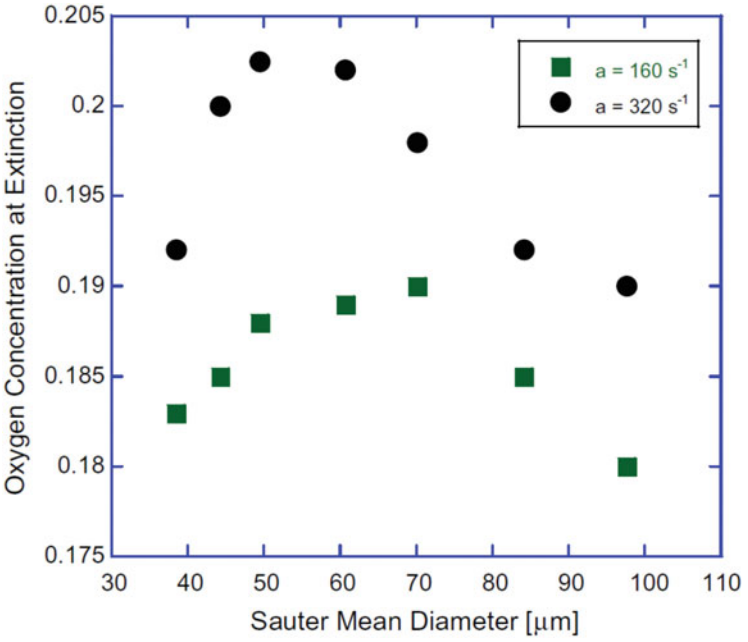

Fig. 19 Dependence of oxygen concentration at extinction on the Sauter mean droplet diameter for two different strain rates ($Y_w = 0{:}022$) [26]

also observed that for water vapor mole fraction of 0.2 or more, no flame can be established further.

There is a handful of literature present which have investigated the effect of water droplets as a fire suppressing agent using stagnation flow configuration. These experimental and numerical studies have revealed important characteristics such as the effect of water droplet size distribution, in case of poly dispersed water spray, on the laminar flame speed. Yang and Kee [36] have presented a computational model to describe two phase interactions between freely propagating premixed methane-air flame and mono-dispersed water droplets using commercial PREMIX code. The gas phase, which includes detailed chemistry, was modeled using adaptive Eulerian mesh whereas the discrete droplets were represented by the Lagrangian frame. It was observed that water droplets below the critical size (10 μm) is ineffective to further affect the extinction process of methane-air flame. The model also predicted turning-point extinction behavior for larger droplets.

Modak et al. [37] have studied numerically, using PREMIX code, the influence of fine water mist on the suppression of laminar freely propagating strain-free premixed methane-, propane-, hydrogen-air flames in atmospheric pressure. It was observed that smaller size droplets are more effective than larger droplets which are already concluded previously by many others experimentally and numerically. The critical small diameter limit was observed to be 10 μm (for methane-air and propane-air)

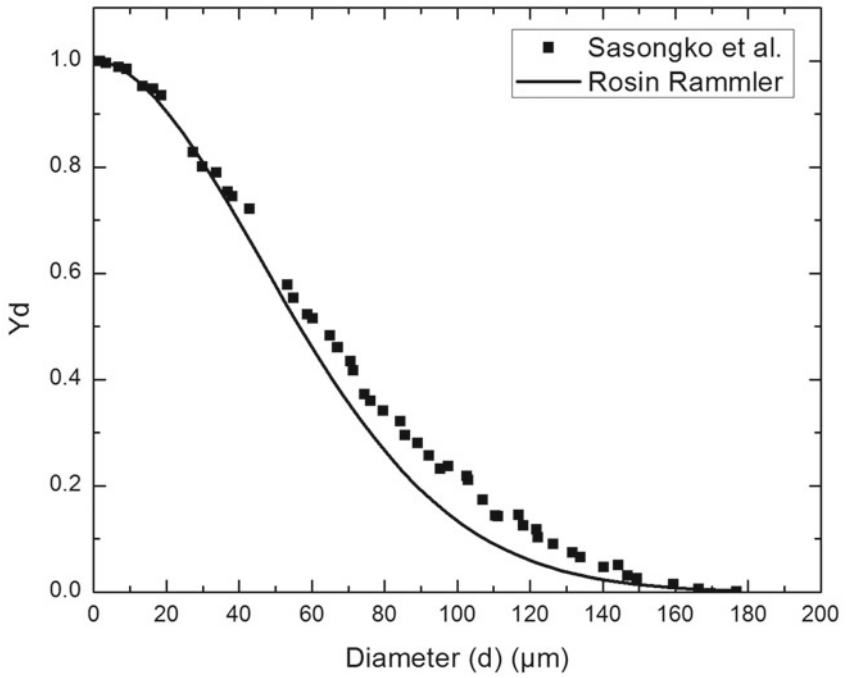

Fig. 20 Rosin Rammler curve fits to experimental droplet distributions

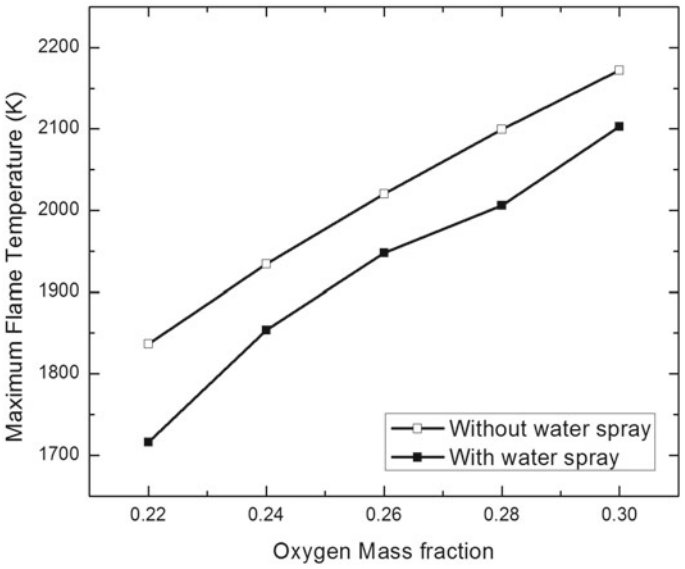

Fig. 21 Comparison of maximum flame temperature

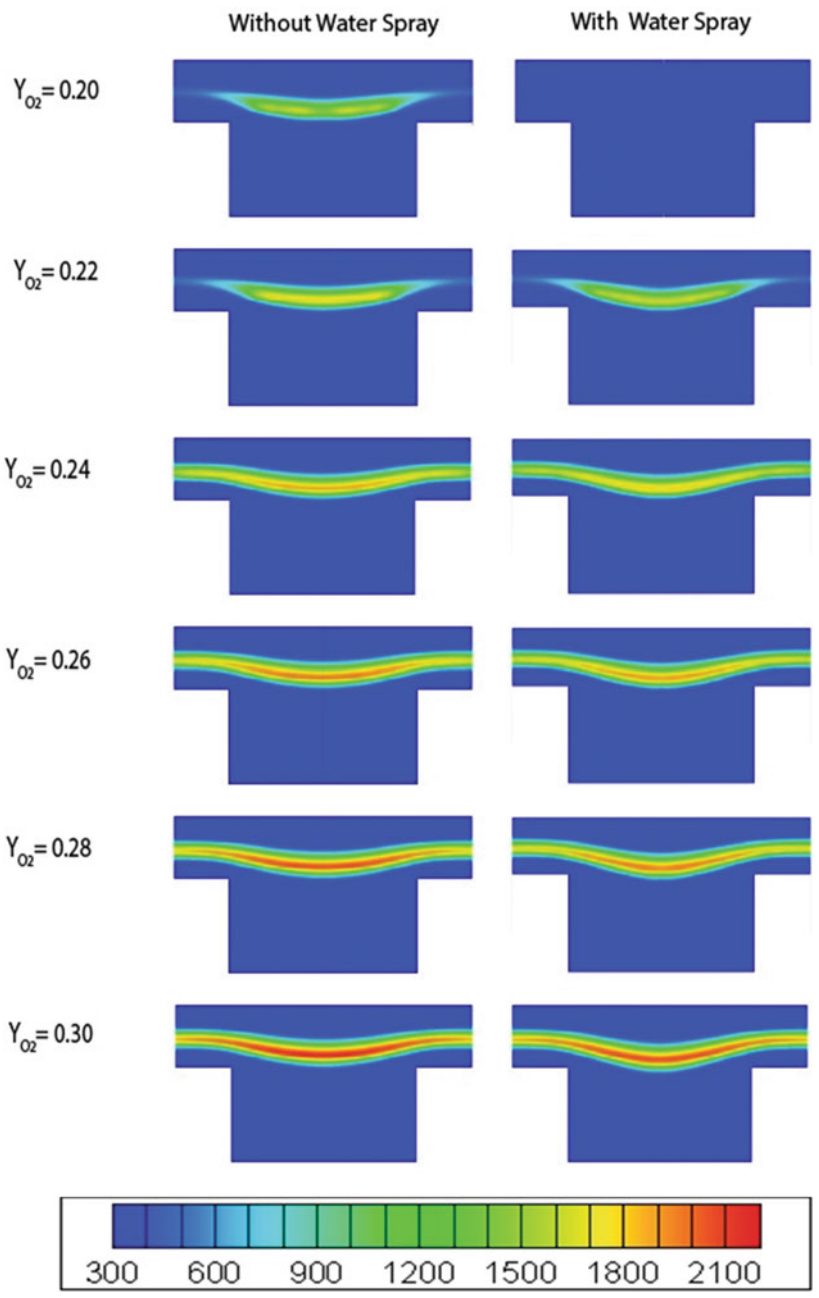

Fig. 22 Comparison of temperature contour

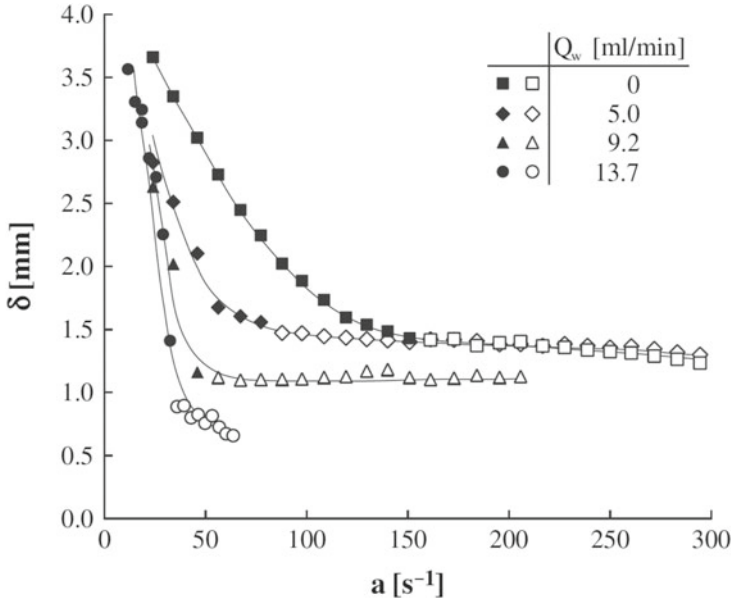

Fig. 23 Variation of flame thickness with strain rate [28]

and 2 μm (for hydrogen-air) below which there is no further influence on the droplet size which is in agreement with the analysis of Yang and Kee. 30 μm was denoted as turning-point extinction where burning velocity for methane-air and propane-air was observed to be half of the burning velocity without any water droplets.

Reduction of flammability region of hydrogen-air mixture by using cold fog nozzles and ultrasonic foggers was experimented by Jones et al. [38]. It was concluded that effect of water mist is strongly dependent on the droplet size distribution and the effect is more pronounced for very fine water mist diameters less than 10 μm. The experiment was conducted mainly for nuclear waste storage plant after decommissioning where significant hydrogen generation could occur.

Ingram et al. [39] have studied laminar flame speed for a premixed hydrogen-oxygen-nitrogen mixture using nozzle burner setup and have used water mist with NaOH additive. It was observed that above a critical concentration of water with NaOH additive (SMD ~4 μm), sudden significant reduction in burning velocity occurred. It is concluded that addition of NaOH helps to chemically inhibit the combustion in addition to the evaporative cooling effect due to the addition of water mist.

Joseph et al. [40] have presented a simple lumped parameter approach to study thermodynamic aspects of the interaction between water droplets and hydrogen-air flames in a closed container. The final pressure and temperature variation due to the addition of water can not only suppress the fire; sometimes the addition of water mist could over pressurize the vessel and could create turbulence effect which

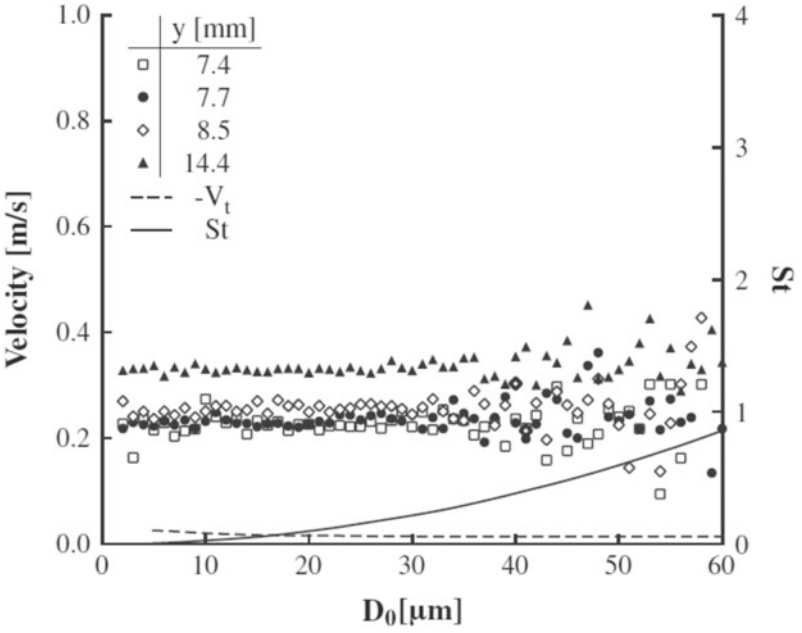

Fig. 24 Droplet velocity, Stokes number and thermophoretic velocity for $a = 80\ s^{-1}$ and $Q_w = 7.33$ ml/min [28]

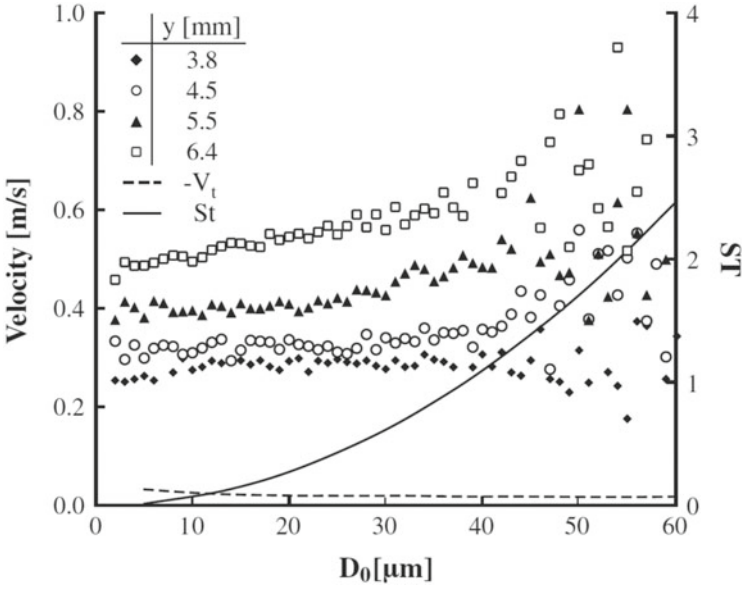

Fig. 25 Droplet velocity, Stokes number and thermophoretic velocity for $a = 230\ s^{-1}$ and $Q_w = 7.33$ ml/min [28]

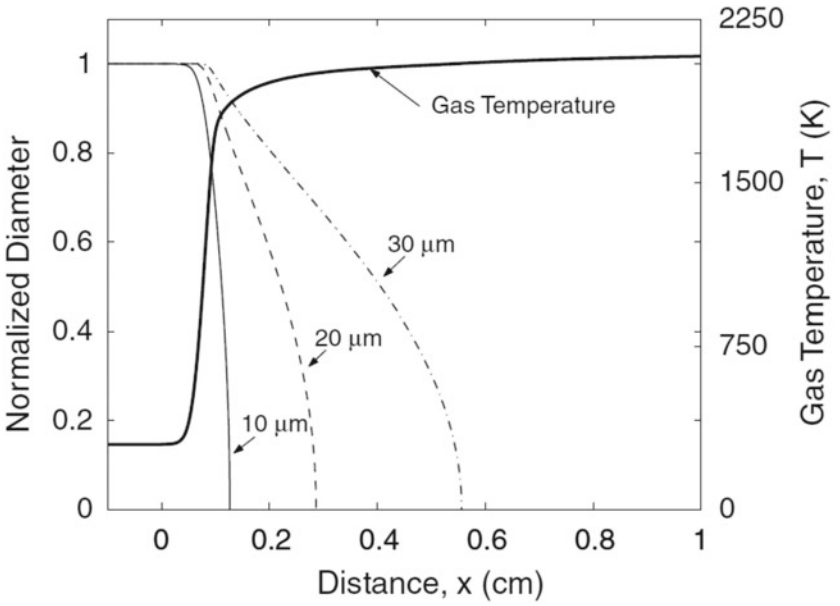

Fig. 26 Variation of normalized droplet diameter across the premixed flame structure, for different initial droplet sizes. Also shown is the gas-phase temperature versus distance [23]

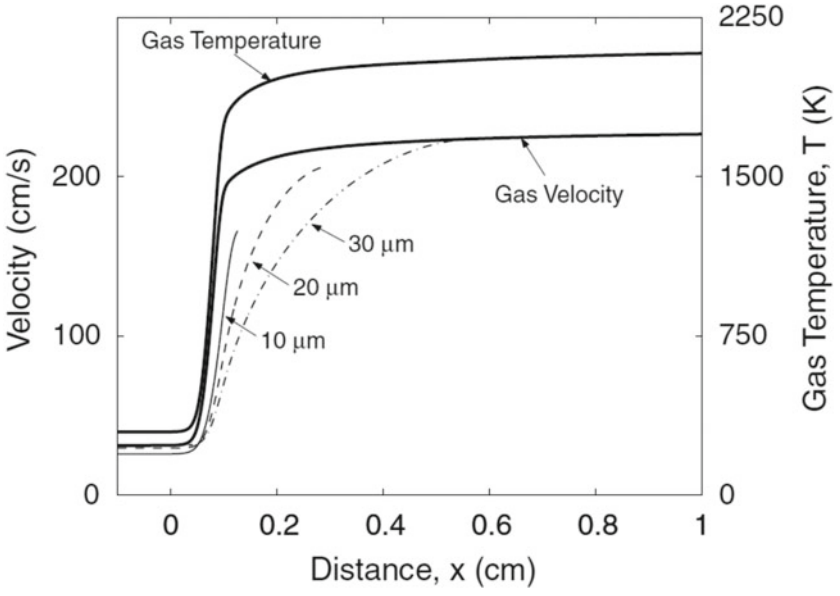

Fig. 27 Comparison of the gas and droplet velocity across the premixed flame structure, for different initial droplet sizes. Also shown is the gas-phase temperature versus distance [23]

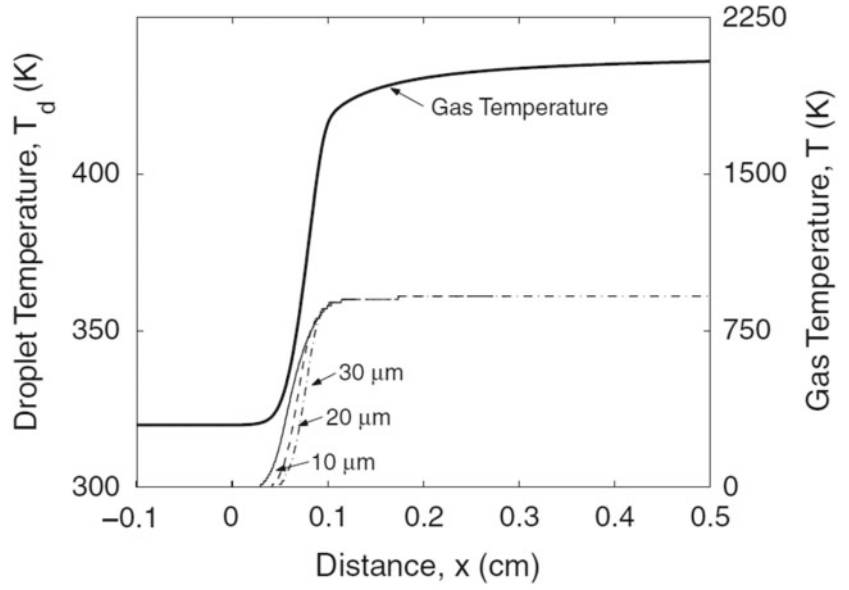

Fig. 28 Comparison of gas and droplet equilibrium temperature (T_{equil}) across the premixed flame structure, for different initial drop sizes [23]

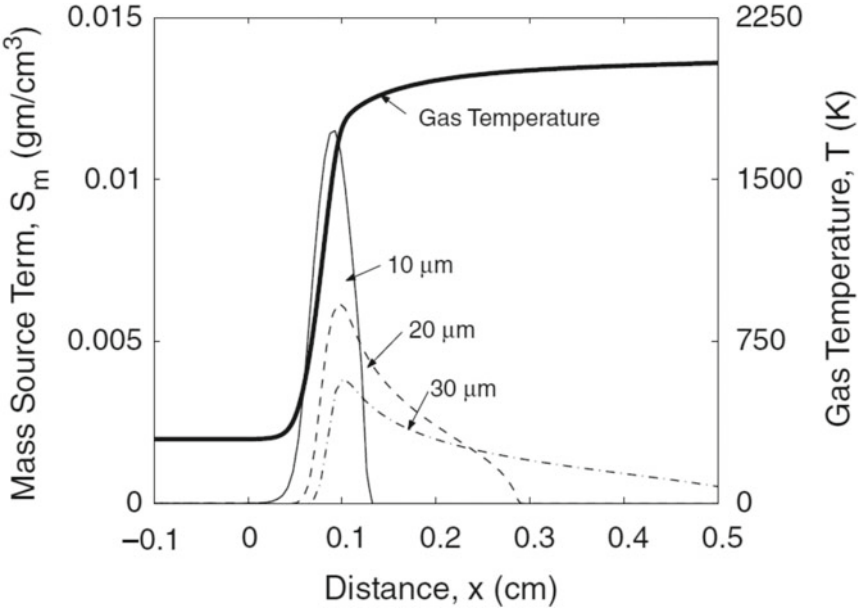

Fig. 29 The mass source term (S_m) across the premixed flame structure, for different initial droplet sizes and $Y_0 = 0.02$. Also shown is the gas-phase temperature profile [23]

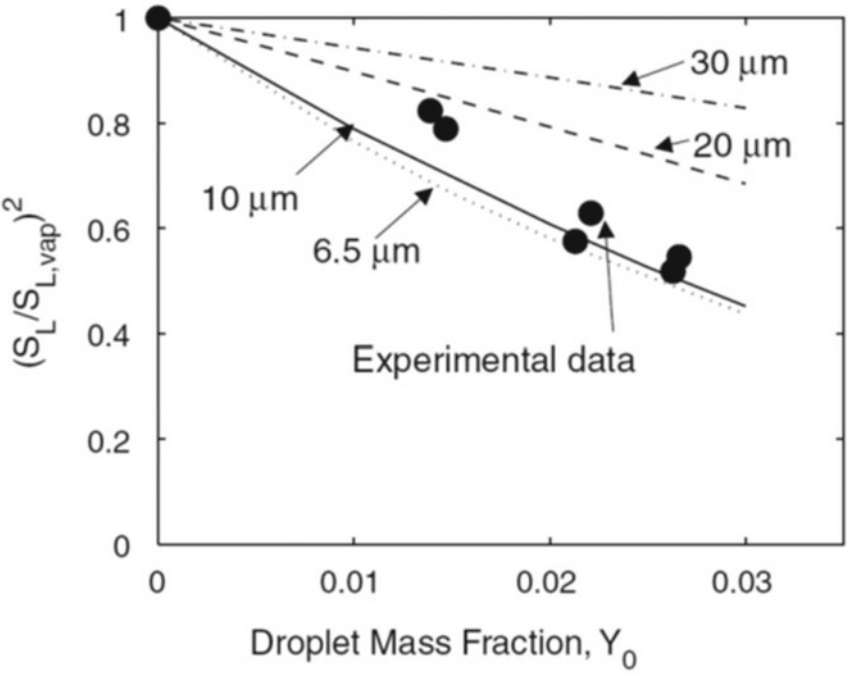

Fig. 30 Variation of the flame strength of a premixed flame versus droplet mass fraction, for different initial drop sizes [34]

would eventually enhance the flame propagation. The lumped parameter approach can only predict the final pressure and temperature in case of addition of water mist to the hydrogen-air flame. It was concluded that although liquid water acts as a heat sink, steam generated due to vaporization of liquid water in the reaction zone becomes important when hydrogen concentration attains certain critical value. The final pressure, in that case, becomes higher than the final pressure that would have attained without liquid water addition.

Cheikhravat et al. [41] have observed that in standard atmospheric pressure and temperature, the addition of water mist to the dry hydrogen/air mixture did not shift the lower flammability limit until a critical droplet density number was reached. The experiment was done in a spherical constant volume vessel and it was observed that for larger droplet size with Sauter mean diameter (SMD) in the range of 200–250 μm, effect of water spray on the flame speed is negligible. With water droplet diameter less than 10 μm, violence of explosion was mitigated due to reduction of flame speed; however opposite effect was observed for very lean hydrogen/air mixture (10% mole fraction of H_2) as the turbulence effect was enhanced by addition of droplets in this case and it helped to complete the combustion.

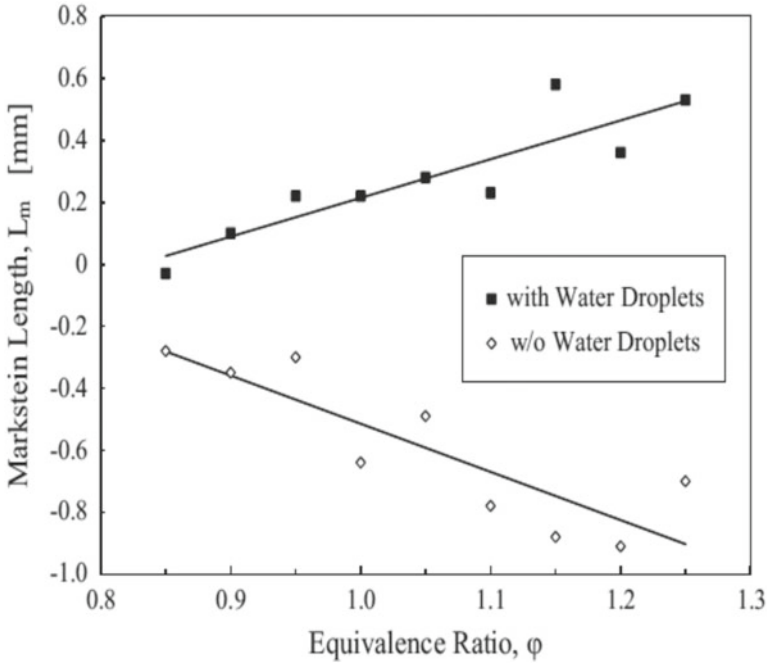

Fig. 31 Markstein length with and without water droplets [34]

5.3 Flame Acceleration

Munshi et al. [42] numerically studied effects of polydisperse water spray in hydrogen air premixed flame. A stagnation jet plate configuration was chosen for flame speed determination. Stabilized flames in different stretch conditions are now introduced with polydisperse water spray of different number mean diameters. Figure 32 depicts flame speed normalized with respect to the flame speed in absence of spray and flame temperature normalized with respect to flame temperature in absence of spray respectively with an initial flame stretch of 270.7 s^{-1}. For the stretch mentioned, it can be clearly observed to increase the flame speed and temperature for a certain range of spray mass loading. The only difference, in the two different stretch scenarios, is that the inlet velocity in case of lower stretch is 4 m/s whereas for the highest stretch it is 7 m/s. Due to increase in the velocity, flow Reynolds number is increased in case of higher inlet velocity condition giving rise to the turbulence in the flow field in presence of water spray. At this situation momentum and mass transfer take place in case of droplets interacting with the continuous phase, which eventually could lead to a turbulization of the flow field when two-way turbulence coupling is considered. This is the predominant physics which is significant in interpreting the phenomenon

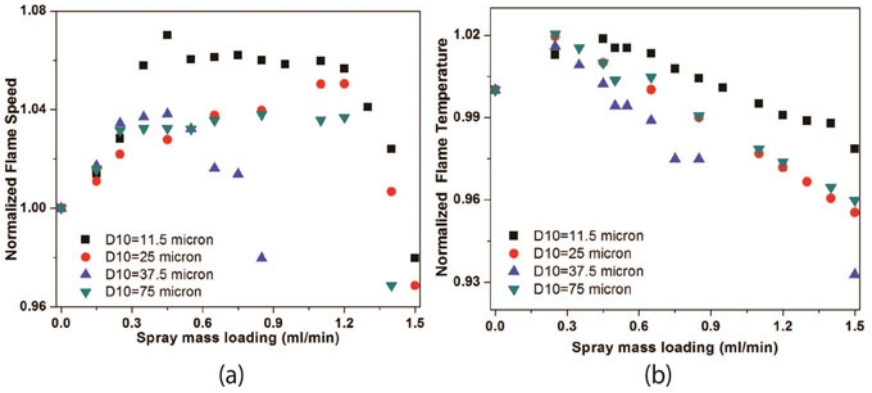

Fig. 32 Effect of spray on flame speed (**a**) and temperature (**b**) for stretch = 270.7 s^{-1}

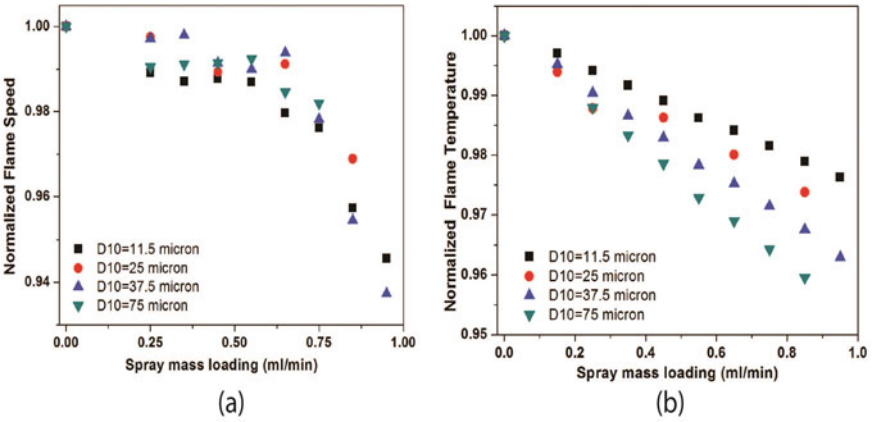

Fig. 33 Effect of spray on flame speed (**a**) and temperature (**b**) for stretch = 125.2 s^{-1}

depicted in Figs. 32 and 33. Figure 33 shows that at low stretch of 125.2 s^{-1} this flame acceleration is absent due to low gas phase velocity. This is due to the fact that, once the stretch is higher than a transition point, turbulization effect of spray surpasses the evaporative effect and instead of flame extinction due to heat loss by evaporation, flame accelerates due to turbulence.

6 Summary and Recommendations for Future Research

In this chapter, an overview of the interaction of flame and water spray was presented. Different simple laboratory scale flames were used to investigate the effects of water

spray. Significant experimental and numerical works are summarized for both premixed and non-premixed flame. Counter flow burner was found to be majorly used configuration to study the effects of water spray in non-premixed flame. It is clearly understood that droplet size significantly affects the flame water spray interaction. Droplet inertia and evaporation are the two phenomena which govern the flame suppression. An optimum droplet diameter is found for which effectiveness of the water spray is maximum. Flame speed is influenced by the presence of water spray for the premixed flame. A decrement of flame speed observed due to evaporation heat loss of the droplets. It is also found that flame speed increases for hydrogen air premixed flame in presence of fine water droplets at high stretch rate. Turbulization effect which is caused by droplet-gas phase interaction is identified as a cause for flame acceleration.

References

1. G. Grant, J. Brenton, D. Drysdale, Fire suppression by water sprays. Prog. Energy Combust. Sci. **26**, 79–130 (2000)
2. R. Mugele, H.D. Evans, Droplet size distribution in sprays. Ind. Eng. Chem. **43**, 1317–1324 (1951)
3. S.R. Turns, *An Introduction to Combustion: Concepts and Applications*, 2nd edn. (The McGraw-Hill Companies Inc, USA, 2000)
4. H. Tsuji, Counterflow diffusion flames. Prog. Energy Combust. Sci. **8**, 93–119 (1982)
5. M.D. Smooke, R.A. Yetter, T.P. Parr, D.M. Hanson-Parr, M.A. Tanoff, M.B. Colket, R.J. Hall, Computational and experimental study of ammonium perchlorate/ethylene counterflow diffusion flames. Proc. Combust. Inst. **28**, 2013–2020 (2000)
6. M.D. Smooke, I.K. Puri, and K. Seshadri, A comparison between numerical calculations and experimental measurements of the structure of a counterflow diffusion flame burning diluted methane in diluted air, in *Twenty-First Symposium (International) on Combustion*, vol. 21, 1988, pp. 1783–1792
7. K. Seshadri, C. Trevino, M.D. Smooke, Analysis of the structure and mechanisms of extinction of a counterflow methanol-air diffusion flame. Combust. Flame **76**, 111–132 (1989)
8. G. Dixon-Lewis, T. David, P.H. Gaskell, S. Fukutani, H. Jinno, J.A. Miller, R.J. Kee, M.D. Smooke, N. Peters, E. Effelsberg, J. Warnatz, F. Behrendt, Calculation of the structure and extinction limit of a methane-air counterflow diffusion flame in the forward stagnation region of a porous cylinder, in *Twentieth Symposium (International) on Combustion Symposium (International) on Combustion*, vol. 20, 1985, pp. 1893–1904
9. G. Dixon-Lewis, V. Giovangigli, R.J. Kee, J.A. Miller, B. Rogg, M.D. Smooke, G. Stahl, J. Warnatz, Numerical modeling of the structure and properties of tubular strained laminar premixed flames. Am. Inst. Aeronaut. Astronaut. **131**, 125–144 (1991)
10. G. Balakrishnan, M.D. Smooke, F.A. Williams, A numerical investigation of extinction and ignition limits in laminar nonpremixed counterflowing hydrogen-air streams for both elementary and reduced chemistry. Combust. Flame **102**, 329–340 (1995)
11. G. Amantini, J.H. Frank, M.D. Smooke, A. Gomez, Computational and experimental study of steady axisymmetric non-premixed methane counterflow flames. Combust. Theory Model. **11**, 47–72 (2007)
12. G. Amantini, J.H. Frank, M.D. Smooke, A. Gomez, Computational and experimental study of standing methane edge flames in the two-dimensional axisymmetric counterflow geometry. Combust. Flame **147**, 133–149 (2006)

13. N. Peters, *Laminar flamelet concepts in turbulent combustion*, in *Symposium (International) on Combustion*, vol. 21, 1988, pp. 1231–1250
14. N. Peters, Laminar diffusion flamelet models in non-premixed turbulent combustion. Prog. Energy Combust. Sci. **10**, 319–339 (1984)
15. A. Lock, S.K. Aggarwal, I.K. Puri, Effect of fuel type on the extinction of fuel and air stream diluted partially premixed flames. Proc. Combust. Inst. **32**, 2583–2590 (2009)
16. J.S. Park, D.J. Hwang, J. Park, J.S. Kim, S. Kim, S.I. Keel, T.K. Kim, D.S. Noh, Edge flame instability in low-strain-rate counterflow diffusion flames. Combust. Flame **146**, 612–619 (2006)
17. A. Lock, S.K. Aggarwal, I.K. Puri, U. Hegde, Suppression of fuel and air stream diluted methane–air partially premixed flames in normal and microgravity. Fire Saf. J. **43**, 24–35 (2008)
18. A. Lock, A.M. Briones, S.K. Aggarwal, I.K. Puri, U. Hegde, Liftoff and extinction characteristics of fuel- and air-stream-diluted methane–air flames. Combust. Flame **149**, 340–352 (2007)
19. A.J. Lock, A.M. Briones, X. Qin, S.K. Aggarwal, I.K. Puri, U. Hegde, Liftoff characteristics of partially premixed flames under normal and microgravity conditions. Combust. Flame **143**, 159–173 (2005)
20. A.M. Lentati, and H.K. Chelliah, Physical, thermal, and chemical effects of fine-water droplets in extinguishing counterflow diffusion flames, in *Symposium (International) on Combustion*, vol. 27, 1998, pp. 2839–2846
21. E.J.P. Zegers, B.A. Williams, R.S. Sheinson, J.W. Fleming, Dynamics and suppression effectiveness of monodisperse water droplets in non-premixed counterflow flames. Proc. Combust. Inst. **28**, 2931–2937 (2000)
22. A.M. Lentati, H.K. Chelliah, Dynamics of water droplets in a counterflow field and their effect on flame extinction. Combust. Flame **115**, 158–179 (1998)
23. H.K. Chelliah, A.K. Lazzarini, P.C. Wanigarathne, G.T. Linteris, Inhibition of premixed and non-premixed flames with fine droplets of water and solutions. Proc. Combust. Inst. **29**, 369–376 (2002)
24. A. Dvorjetski, J.B. Greenberg, Theoretical analysis of polydisperse water spray extinction of opposed flow diffusion flames. Fire Saf. J. **39**, 309–326 (2004)
25. S. Pramanik, A. Mukhopadhyay, Numerical study of counterflow diffusion flame and water spray interaction. J. Therm. Sci Eng. Appl. **8**, 011–018 (2014)
26. M.N. Sasongko, M. Mikami, A. Dvorjetski, Extinction condition of counterflow diffusion flame with polydisperse water sprays. Proc. Combust. Inst. **33**, 2555–2562 (2011)
27. S. Sarkar, A. Mukhopadhyay, S. Sen, Numerical study of the effect of fine polydisperse water spray on laminar flame speed of hydrogen/air premixed flames stabilized in the stagnation flow field, in *ILASS-Asia 2016, 18th Annual Conference on Liquid Atomization and Spray Systems—Asia*, Chennai, India
28. A. Yoshida, R. Takasaki, K. Kashiwa, H. Naito, Y. Saso, Extinguishment of counterflow methane/air diffusion flame by polydisperse fine water droplets. Combust. Flame **160**, 1357–1363 (2013)
29. A.K. Lazzarini, R.H. Krauss, H.K. Chelliah, G.T. Linteris, Extinction conditions of non-premixed flames with fine droplets of water and water/NaOH solutions. Proc. Combust. Inst. **28**, 2939–2945 (2000)
30. P.G. Arias, H.G. Im, P. Narayanan, A. Trouvé, A computational study of non-premixed flame extinction by water spray. Proc. Combust. Inst. **33**, 2591–2597 (2011)
31. F. Takahashi, V.R. Katta, Extinguishment of diffusion flames around a cylinder in a coaxial air stream with dilution or water mist. Proc. Combust. Inst. **32**, 2615–2623 (2009)
32. C.C. Ndubizu, R. Ananth, P.A. Tatem, V. Motevalli, On water mist fire suppression mechanisms in a gaseous diffusion flame. Fire Saf. J. **31**, 253–276 (1998)
33. G. Liao, J. Liu, J. Qin, B. Yao, Experimental study on the interaction of fine water spray with liquid pool fires. J. Therm. Sci. **10**, 377 (2001)
34. A. Yoshida, T. Okawa, W. Ebina, H. Naito, Experimental and numerical investigation of flame speed retardation by water mist. Combust. Flame **162**, 1772–1777 (2015)

35. C.K. Law, P. Cho, M. Mizomoto, H. Yoshida, Flame curvature and preferential diffusion in the burning intensity of bunsen flames, in *Twenty-First Symposium (International) on Combustion*, vol. 21, 1988, pp. 1803–1809
36. W. Yang, R.J. Kee, The effect of monodispersed water mists on the structure, burning velocity, and extinction behavior of freely propagating, stoichiometric, premixed, methane-air flames. Combust. Flame **130**, 322–335 (2002)
37. A.U. Modak, A. Abbud-Madrid, J.-P. Delplanque, R.J. Kee, The effect of mono-dispersed water mist on the suppression of laminar premixed hydrogen–, methane–, and propane–air flames. Combust. Flame **144**, 103–111 (2006)
38. A. Jones, P.F. Nolan, Discussions on the use of fine water sprays or mists for fire suppression. J. Loss Prev. Process Ind. **8**, 17–22 (1995)
39. J.M. Ingram, A.F. Averill, P.N. Battersby, P.G. Holborn, P.F. Nolan, Suppression of hydrogen–oxygen–nitrogen explosions by fine water mist: Part 1 Burning velocity. Int. J. Hydrog. Energy **37**, 19250–19257 (2012)
40. C. Joseph-Auguste, H. Cheikhravat, N. Djebaïli-Chaumeix, E. Deri, On the use of spray systems: An example of R&D work in hydrogen safety for nuclear applications. Int. J. Hydrog. Energy **34**, 5970–5975 (2009)
41. H. Cheikhravat, J. Goulier, A. Bentaib, N. Meynet, N. Chaumeix, C.E. Paillard, Effects of water sprays on flame propagation in hydrogen/air/steam mixtures. Proc. Combust. Inst. **35**, 2715–2722 (2015)
42. J. Munshi, S. Sarkar, S. Sen, A. Mukhopadhyay, Numerical study of the effect of fine polydisperse water spray on laminar flame speed of hydrogen/air premixed flames stabi-lized in the stagnation flow field, in *ILASS-Asia 2016*, *18th Annual Conference on Liquid Atomization and Spray Systems—Asia*, Chennai, India